Brightness enhancement on a narrow linewidth FBG-based MOPA fiber laser

Tian Xin[1,2,3,†], Binyu Rao[1,2,3,†], Meng Wang[1,2,3], Xiaoming Xi[1,2,3,4*], Zhixian Li[1,2,3], Zilun Chen[1,2,3], Hu Xiao[1,2,3], Pengfei Ma[1,2,3], Zefeng Wang[1,2,3,5*]

[1] *College of Advanced Interdisciplinary Studies, National University of Defense Technology, Changsha 410073, China*

[2] *Nanhu Laser Laboratory, National University of Defense Technology, Changsha, 410073, China;*

[3] *State Key Laboratory of Pulsed Power Laser Technology, Changsha, 410073, China;*

[4]*E-mail: exixiaoming@163.com*

[5]*E-mail: zefengwang_nudt@163.com*

[†]*These authors contributed equally to this paper*

*Correspondence to: X. Xi, Email: exixiaoming@163.com
Z. Wang, Email: zefengwang_nudt@163.com

Abstract In this paper, we have experimentally demonstrated a high power and high brightness narrow-linewidth fiber amplifier seeded by an optimized fiber oscillator. In order to improve the temporal stability, the fiber oscillator consists of a composite FBG-based cavity with an external feedback structure. By optimizing the forward and backward pumping ratio, nonlinear effects and SRS-induced mode distortion of the fiber amplifier

This peer-reviewed article has been accepted for publication but not yet copyedited or typeset, and so may be subject to change during the production process. The article is considered published and may be cited using its DOI.

10.1017/hpl.2024.25

are suppressed comprehensively, accompanying with the simultaneous improvement of beam quality and output power. The laser brightness is enhanced further by raising the threshold of transverse mode instability by ~1.0 kW by coiling the gain fiber with a novel curvature shape. Finally, a 6 kW narrow linewidth laser is achieved with beam quality (M^2) of ~1.4. The laser brightness has doubled comparing to the results before optimization. To the best of our knowledge, it is the highest brightness narrow linewidth fiber laser based on one-stage MOPA structure.

Key words: *brightness, fiber laser, narrow linewidth, Ytterbium-doped fiber*

I. INTRODUCTION

In recent years, fiber lasers have developed towards higher power, higher brightness, and wider applications owing to their compact structure, high conversion efficiency, excellent beam quality and convenient thermal management [1-3]. From the perspective of power scaling of fiber lasers, the pursuit of even higher power is never satisfied. However, the ultimate output power is challenged by transverse mode instability (TMI) and fiber nonlinearities resulted from the increase of density within fiber core and long interaction length [4-7]. Besides, the beam quality has to been sacrificed with larger fiber core for higher power and weaker nonlinear effects. The emergence of both spectral beam combination (SBC) and coherent beam combination (CBC) provides promising methods to break through the limitations of fiber lasers while maintaining good beam quality [8-11]. The power scaling ability of combination systems is dependent on the input power and the number of sub beam combined. Laser brightness, which can be defined as $\beta \propto P/(M^2)^2$, is an extremely important parameter for application of SBC

https://doi.org/10.1017/hpl.2024.25 Published online by Cambridge University Press

and CBC, where P is output power and M^2 is beam quality factor [3]. Thus, developing high brightness narrow linewidth fiber amplifier (NLFA) is critical and highly desired for beam combination technology.

Master oscillator power amplification (MOPA) structure is typically used to realize NLFA. These fiber amplifiers mainly adopt two types of seed: phase modulated single frequency laser and fiber oscillator laser. The high-power fiber laser with linewidth less than 10 GHz is useful for CBC, which can be achieved by the MOPA structure seeded by phase modulated single frequency laser and has reached to 2 kW level currently [12-14]. It is usually limited by stimulated Brillouin scattering (SBS) effect during the power scaling due to ultra-narrow linewidth [15, 16]. The higher power laser with linewidth less than 1 nm have also been intensively researched, which is useful for SBC system whose linewidth requirements are not as strict as CBC. The power scaling of such high power NLFAs is affected by TMI and various nonlinear effects including SBS, stimulated Raman scattering (SRS) and four-wave mixing (FWM) [17-23]. In 2022, Ma et al. reported a 7.03 kW near single mode NLFA with 3 dB linewidth of 0.76 nm, which is based on the phase modulated single frequency laser seed [19]. However, the recorded output power of high brightness NLFA based on fiber oscillator laser seed is no more than 5 kW level [20-23]. The highest reported power is 4.6 kW with 3 dB linewidth of 0.35 nm and M^2 factor of 1.31 [23]. The phase modulated single frequency laser seed maintains good properties of single frequency but has to use a complex multi-stages amplification configuration. Fiber oscillator laser seed has advantages of simple one-stage structure, good robustness, and low cost but need to overcome nonlinear effects induced by temporal instability. With optimizing the time domain features of seed and suppressing nonlinear

https://doi.org/10.1017/hpl.2024.25 Published online by Cambridge University Press

effects and TMI comprehensively, NLFA seeded by fiber oscillator is a potential method with good cost-performance.

In this paper, we demonstrate a bidirectional pumping NLFA seeded by a fiber oscillator. The fiber oscillator is based on a composite cavity with external feedback structure for good temporal stability. By optimizing the bi-directional pumping ratio, the various nonlinear effects are suppressed comprehensively, and the output power combined with beam quality are improved. Furthermore, the TMI threshold is also improved by ~1.0 kW by coiling the gain fiber with a novel curvature shape. Finlay, a 6 kW narrow linewidth output is achieved with an optical-to-optical efficiency of 85.0%. The 3 dB and 20 dB linewidth are 0.63 nm and 2.81 nm, respectively. The beam quality is measured to be M^2~1.4 and the signal to Raman ratio is more than 30 dB at the maximum output power. The laser brightness has doubled comparing to the results before optimization. To the best of our knowledge, this is the reported output power record based on this narrow linewidth one-stage MOPA fiber laser.

II. OPTIMIZATION FOR SEED STRUCTURE

It has been reported that many strategies, such as a large core, short length gain fiber, a backward pumping structure and a wavelength stabilized laser diode (WS LD) can be used to decrease the linewidth of fiber oscillators [22]. However, even if these methods are employed, self-pulsing and poor temporal characteristics are inevitable when running into narrow linewidth fiber oscillators. The narrower bandwidth of the FBG, the greater temporal fluctuations of fiber oscillator laser. Moreover, the seed laser with high peak power self-pulses would lead to a much lower SRS threshold during the power amplification [24-26]. Thus, enhancing temporal stability of the seed is the key for high power NLFA system.

https://doi.org/10.1017/hpl.2024.25 Published online by Cambridge University Press

Some methods have been studied for improving temporal characteristics of fiber oscillator, such as either a composite cavity or external feedback [27-31]. Here, we proposed a novel hybrid structure to combine these two methods, whose schematic diagram is depicted in Fig. 1. Different from conventional F-P structure, the fiber oscillator can be treated as a composite cavity with external feedback. The composite cavity that utilizing an additional low-reflectivity (LR) FBG with wide bandwidth (WB) outside the oscillator cavity has been reported to improve the temporal stability of fiber oscillator laser [27]. However, additional WB-LR FBG contains more longitudinal modes in itself and thus it is not suitable for our narrow linewidth laser system. Besides, using additional narrow bandwidth (NB) LR FBG to form a composite cavity is also inappropriate because a slightly mismatch of the center wavelength between the two NB-LR FBGs would results in the failure of this strategy, especially when they experience different thermal loads. Therefore, a modified composite cavity with an additional high reflectively (HR) FBG rather than LR FBG is adopted in this paper. The theoretical analysis could refer to Ref. [28]. The longitudinal modes of a composite cavity are the combined longitudinal modes with different frequency components from the separate cavity. Simulation results show the peak and valley points in the temporal intensity of the two frequency components could cancel each other. Therefore, the temporal fluctuations of the combined two frequency components are less than a separate frequency component. Besides, the composite cavity could help select the longitudinal modes with the same frequency so that it reduces the crosstalk between longitudinal modes. In this way, the temporal fluctuations of the seed could be reduced.

https://doi.org/10.1017/hpl.2024.25 Published online by Cambridge University Press

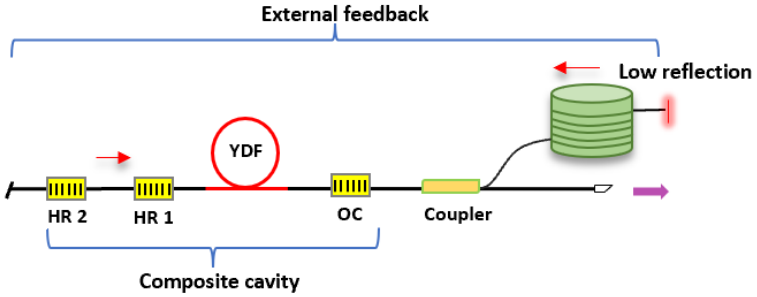

Figure 1. A schematic of the novel cavity.

Besides, it has been reported that the peak intensity of the self-pulses can be weakened and temporal properties can be enhanced after laser transmitting over long passive fibers [29]. However, the signal light injecting amplifier directly would bring about decrease of the SRS threshold and spectral broadening in fiber laser system. Here, the long passive fiber is introduced neither in the cavity nor between the seed and the amplifier. As showed in Fig. 1, the novel structure utilizes an optical coupler with one arm of the coupler to connect the long passive fiber and the other arm connect to the amplifier. It is worth to note that the output fiber is not cleaved to 8° but a flat angle (0°), which means that there is a ~4% signal light at the fiber end reflected into the modified composite cavity. The introduced weak light is generated from the Fresnel reflection and forms external feedback of the fixed cavity. The feedback light with stable temporal features would affect the temporal features of the longitudinal modes in the cavity, which is different from random fiber laser (RFL) with modeless spectrum [30]. The use of long fibers feedback in the MOPA system helps to reduce the pulses intensity by nonlinear effects. When the signal laser transmitting over the long passive fibers, the high intensity self-pulses would be split into low intensity pulses due to SPM effect [31]. Then, the average pulse intensity and temporal fluctuations of the signal could decrease simultaneously. Moreover, the feedback from Fresnel reflection can be also treated as a composite cavity possessing additional LR FBG

https://doi.org/10.1017/hpl.2024.25 Published online by Cambridge University Press

with super wide bandwidth, which is also helpful to seed stability [27,32]. The effect can be superimposed on long fibers feedback. Essentially, the two methods both break the original coherence characteristics between effective longitudinal modes and reduce the intensity and gradient distribution of self-pulses. The temporal features of the seed structure could be enhanced reasonably.

Although the temporal characteristics could be optimized, the influence of seed structure on linewidth need to be taken in. Because the feedback light from the Fresnel reflection transmits through long passive fiber, the spectrum of seed laser contains the features of feedback light. The 3 dB linewidth of output laser between the optimized cavity and traditional cavity without long fibers feedback is almost identical for the limitation of narrow bandwidth FBG, but the bottom of signal spectrum is broadened. More importantly, the rate of spectral broadening is different when the two types of the signal laser are amplified respectively. The optimized seed possesses good temporal features so that the spectral broadening effect is weak and the spectral shape can be maintained well, avoiding spectral bottom broadening severely at high power level [30].

III. EXPERIMENTAL SETUP

Figure 2 demonstrates the experimental structure based on the optimized seed. A WS LD with center wavelength of 976 nm is used as pump source of seed. The HR-FBG 1 and HR-FBG 2 provide reflectivity of ~99.5% and 50% respectively with same full width at half maximum (FWHM) of ~3 nm. The adopted gain fiber is a double-clad ytterbium-doped fiber (YDF), which have a size of 20/400 μm and a length of ~6 m. The absorption coefficient is ~0.55 dB/m at 915 nm. The output coupler (OC) FBG has a reflectivity of ~10% and a FWHM of ~0.05 nm. The pump light is backward injected via a side pump and signal combiner (SPSC). The residual pump

https://doi.org/10.1017/hpl.2024.25 Published online by Cambridge University Press

light is removed by a cladding light stripper (CLS 1). The seed power could provide signal power about 45 W. After the CLS, a 50:50 optical coupler is located after the composite cavity. Half of the power is injected into a long passive fiber with length of ~200 m. The end of passive fiber is cleaved to a flat angle, thus a Frensel feedback light is reflected into the modified cavity. The other output arm of the coupler is connected to the main amplifier through a BPFC. Apart from filtering the spectral noise of injected laser, the BPFC is also performed as a SBS monitor by measuring the backward power at port 3. Another CLS is attached after the BPFC in order to remove the residual pump power of the amplifier.

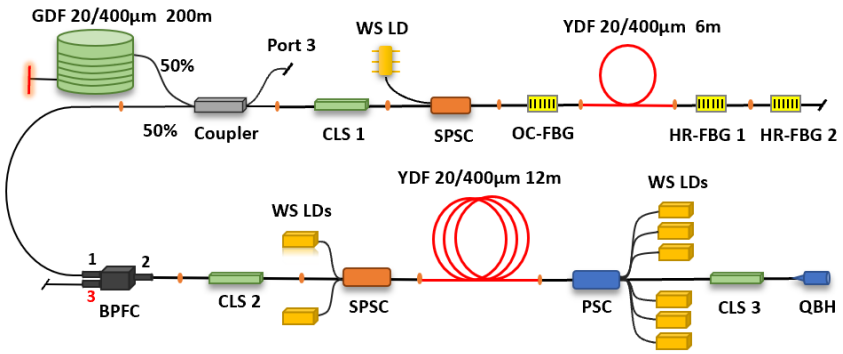

Figure 2. Schematic of the narrow-linewidth MOPA fiber amplifier with bidirectional pump structure.

The amplification stage adopts a bidirectional pump structure. The pump source employs eight groups of 976 nm WS LDs with the maximum pump power of ~1100 W for each. The forward and backward pump power were injected via a (2+1) ×1 SPSC and a (6+1) ×1 PSC, respectively. The SPSCs used in the laser system can effectively maintain the beam quality, The signal fiber size of SPSC and gain fiber are both 20/400 μm. The length of the YDF in the amplifier is ~12 m. While the core diameter of signal fiber of PSC increases from 20 μm to 25 μm. Notably, the absorption coefficient of the YDF in amplification stage is ~0.37 dB/m at wavelength of 915 nm, which is different from that used in seed. The lower absorption

https://doi.org/10.1017/hpl.2024.25 Published online by Cambridge University Press

coefficient of the gain fiber is for a convenient thermal management and a higher TMI threshold. A CLS and a quartz block head (QBH) are attached for the output. The laser performance including output power, optical spectrum, beam quality and temporal features of the laser are measured and recorded in the experiments.

IV. BRIGHTNESS ENHANCEMENT BY PUMP RATIO OPTIMZATION

To improve the laser brightness, the performance of the NLFA is investigated with different bi-directional pumping ratios. The seed power injected into the amplifier is about 20 W with the measured beam quality of M^2~1.25. The feedback power is measured about 440 mW. During the laser operation, the feedback power could remain stable, which is critical to laser performance. Figure 3 depicts output power and their conversion efficiency at pumping ratios of 1:1.9, 1:3.3 and 1:6.4, respectively. In the process of power amplification, the forward pump power is increased firstly, and then backward pump power is increased until the laser brightness decreases or beam quality degrades. One can conclude from the variation of different color blocks that more backward pump power could be injected while the less forward pumping power is set. And when the forward and backward pumping ratio changes from 1:1.9 to 1:6.4, the final output power improves from 4150 W to 5005 W. Define the optical-optical efficiency as ratio of output power minus input seed power to pump power of amplifier, the value at the maximum laser output is 82.8% with the total pump power of 6020 W.

https://doi.org/10.1017/hpl.2024.25 Published online by Cambridge University Press

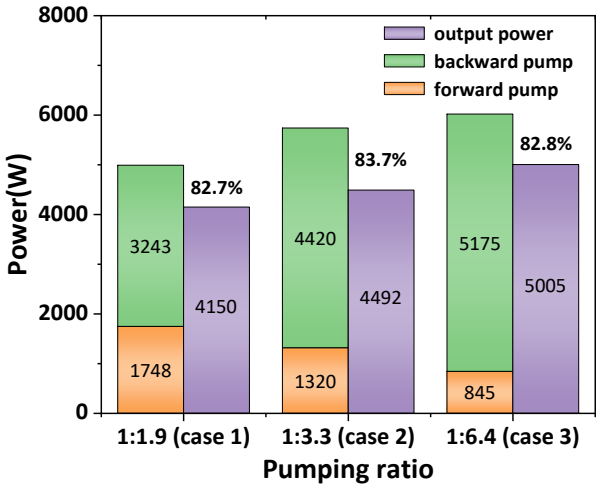

Figure 3. The input and output power and their conversion efficiency at different pumping ratios.

Figure 4 demonstrates the results of output spectra with different pumping ratio. The maximum signal to noise ratio (SNR) can be over 60 dB in the entire spectral range. the output spectra at different powers with forward and backward pumping ratio of 1:1.9 is shown in Fig. 4 (a). Spectral peaks at ~1100 nm caused by FWM effect can be observed once output power exceeded 3 kW. When the output power reached 4150 W, the signal to Raman ratio was about 28.7 dB. Figure 4 (b) shows the output spectra at the condition of pumping ratio of 1:3.3. The output power reached 4492 W at a similar SNR level. Furthermore, the output power exceeded 5 kW when the pumping ratio was further decreased to 1:6.4, and no FWM occurred even at the maximum power, as shown in Fig. 4 (c). These results show that the SRS and FWM effects are mitigated obviously by decreasing the proportion of the forward pump power. In a fiber MOPA amplifier, the forward pumping scheme would result in a higher average signal power along the gain fiber and a longer effective nonlinear length. Therefore, the thresholds of SRS and FWM are reduced with the forward and backward pumping ratio decreasing [21].

https://doi.org/10.1017/hpl.2024.25 Published online by Cambridge University Press

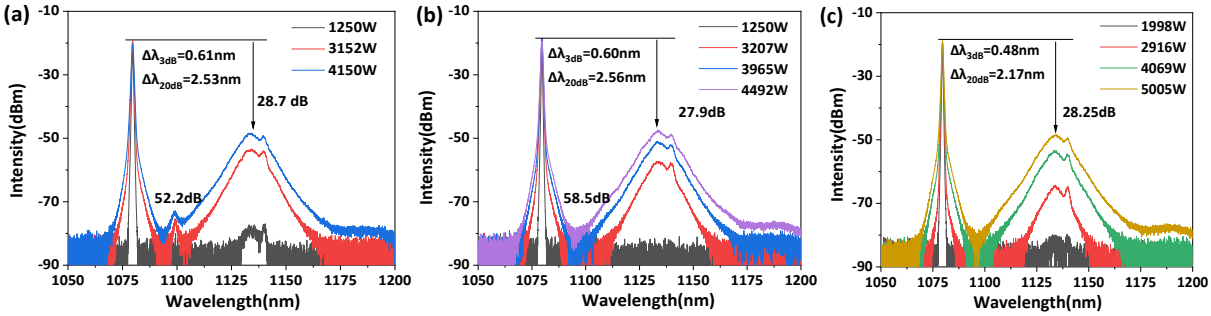

Figure 4. Results of output spectra at different pumping ratios. (a)1:1.9, (b)1:3.3, (c)1:6.4.

Moreover, it is worth noting the variation of signal linewidth versus laser power. With the power increasing, the spectral broadening is the results of self-phase modulation (SPM) and cross-phase modulation effects (XPM) induced by temporal instability of laser. Comparing the final linewidth evolution results among three cases, the 3 dB and 20 dB signal linewidth are reduced from 0.61 nm and 2.53 nm of case 1 to 0.48 nm and 2.1 nm of case 3 respectively. This can also be attributed to a shorter effective length in case 3. Accordingly, the rate of spectral broadening in backward pumping scheme would be slower compared in forward pumping scheme as power scaling. With the forward and backward pump powers injected successively, the linewidth increases at different rates separately. After a relatively low forward pump power injecting, there is a narrower signal linewidth before increasing backward pump power. Then, the signal linewidth grows of three cases at a similar trend with backward pump injecting respectively. Therefore, it's possible to get a narrower linewidth at a higher output power. This process can be depicted clearly according to the evolution of 20 dB linewidth among three cases, as shown in Fig. 5.

https://doi.org/10.1017/hpl.2024.25 Published online by Cambridge University Press

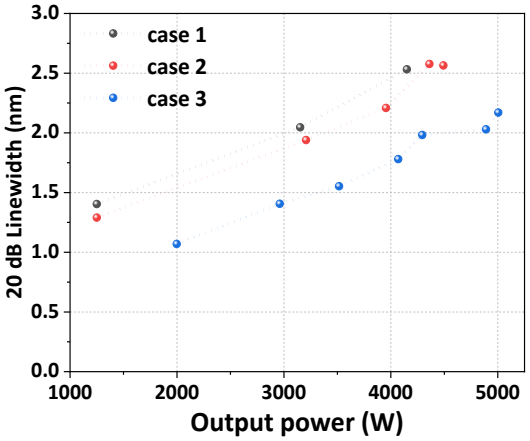

Figure 5. The evolution of 20 dB linewidth versus the output power at different cases.

Among the amplification results of three different pumping ratios, the phenomenon of SRS-induced mode distortion is observed. By calculating spectral integration over the Stokes light, the evolution of SRS ratio and beam quality versus output power are depicted in Fig. 6. It can be seen the increasing trend between SRS ratio and M^2 factor is rather similar in case 1 and 2, which is suggestive of a certain correlation. When Raman ratio exceeds 2%, the beam quality degrades obviously which from near single mode to ~1.7 of M^2 factor. Research shows this SRS-induced mode distortion is attributed to the core-pumped Raman effect. Energy would transfer irreversibly from the fundamental mode (FM) to high-order modes (HOMs) once the Raman light reaches its threshold, contributing to the degradation of beam quality [33]. However, when the power increased above 4500 W in case 3, the M^2 factor didn't increase monotonically with the increase of SRS ratio. This abnormal phenomenon has been observed in Ref. [34] and interpreted as the SRS effect of multimode laser beams. Due to the dynamic change of FM and HOMs at signal wavelength in core-pumped Raman fiber laser, the FM of signal light reached the Raman light firstly as power scaling. When the HOMs of signal light reached its Raman threshold, the HOMs would be consumed and weakened the SRS-induced mode distortion. Once the consuming of HOMs outweighing the generating of HOMs, the M^2 factor would decrease for

https://doi.org/10.1017/hpl.2024.25 Published online by Cambridge University Press

a limited time. One can see that the M^2 factor of 5 kW level NLFA is about 1.35 and the beam quality is almost not deteriorated.

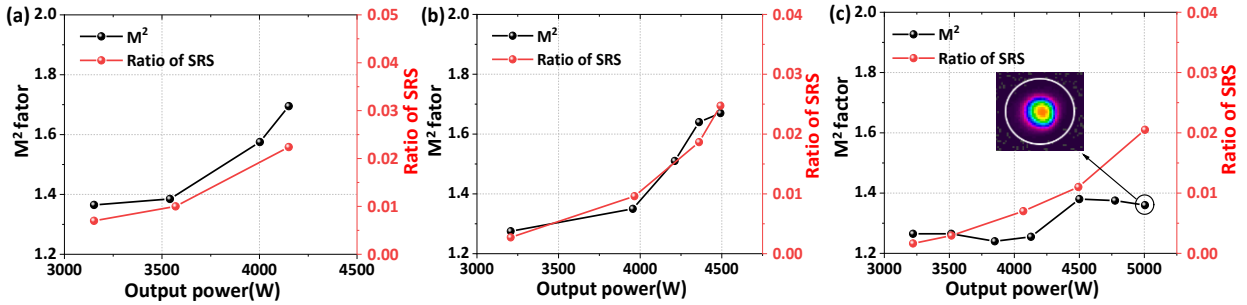

Figure 6. The evolution of ratio of SRS and beam quality versus output power (a) case 1; (b) case 2; (c) case 3 (inset: beam spot at 5005 W).

To further identify the correlation between beam quality and SRS effect, Figure 7 compares the temporal characteristics at the maximum output power with three different pump conditions. It is well known that the sign of TMI is energy transfer at a frequency of kHz level between the FM and the HOMs [35]. By analyzing the time trace from the photodetector (PD) and their corresponding Fast Fourier Transform (FFT) results, there are no signs of TMI in case 1 and case 2. Thus, it can be inferred that the degradation of beam quality results from the SRS effect rather than TMI. For case 3, it is found that the periodical fluctuations of time traces are not obvious but frequencies fluctuations are apparent in the range of 0-5 kHz, indicating that TMI is activated in this fiber amplifier. Based on the results, the TMI threshold can be estimated to be around 5 kW. Considering the capacity of backward pump combiner, the pump power did not increase continuously after the emergence of TMI. For the phenomenon that beam quality could maintain, it can be explained from the increased high order mode loss in the gain fiber induced by coiling. The occurrence of TMI makes the increase of content of high-order modes in fiber core. Owing to the bending loss, the coupled high-order modes leak into the inner cladding of the fiber and

https://doi.org/10.1017/hpl.2024.25 Published online by Cambridge University Press

could be dumped at the CLS regions. Therefore, the abnormal phenomenon of reduced M^2 factor at 5005 W is a result of comprehensive effects of TMI and SRS effect in multimode laser beams.

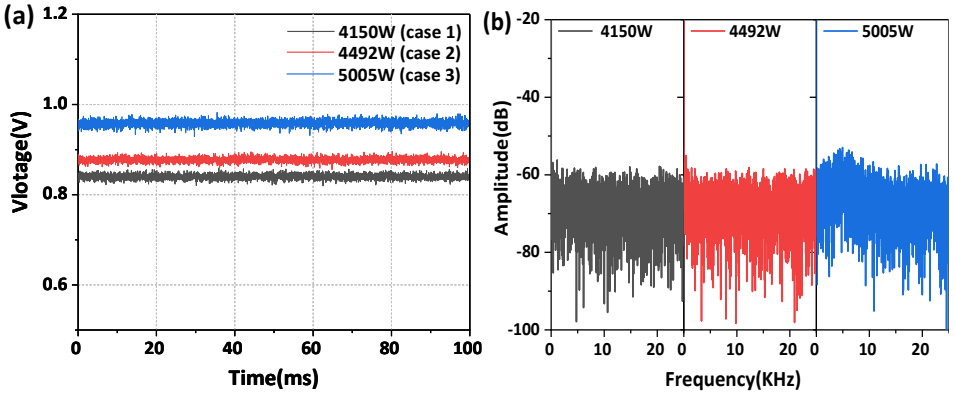

Figure 7. Temporal characteristics at the final output power in three cases. (a) signals of the PD (b) results of FFT

Table 1 summarizes the experimental results of three different pumping ratios. One can conclude that the various nonlinear effects and SRS-induced mode distortion in the amplifier are suppressed comprehensively by adjusting bi-directional pumping ratio, accompanying with an improvement of laser power and laser brightness. The laser brightness is 1.9 times that of the original according to above mentioned formula. The further brightness enhancement is limited by TMI. Actually, it's also urgent to mitigate SRS effect because the Raman light to signal ratio is about to reach the degradation threshold of beam quality.

Table 1. The experimental results with different bi-directional pumping ratios

Case	Output power(W)	Forward/Backward pump power(W)	pumping ratio	3-dB /20-dB linewidth(nm)	SRS ratio	M^2	TMI
1	4150	1748 / 3248	~1:1.9	0.61/2.53	2.2%	1.7	no
2	4492	1320 / 4420	~1:3.3	0.60 / 2.56	2.5%	1.66	no
3	5005	845 / 5175	~1:6.4	0.48 / 2.17	2.0%	1.35	yes

V. BRIGHTNESS ENHANCEMENT BY TMI SUPPRESSION

https://doi.org/10.1017/hpl.2024.25 Published online by Cambridge University Press

To further improve the output power and laser brightness, some designs have to be applied in the NLFA system for mitigating SRS and TMI effects comprehensively. First of all, a home-made integrated output device including PSC, CLS, and QBH without any melting points are reattached after the gain fiber. The fiber length is decreased from 3 m to 1.5 m, which is helpful to weaken SRS effect while maintaining beam quality. Secondly, the coiling shape of the gain fiber is optimized in amplifier for raising the TMI threshold, as shown in Fig. 8. It has been reported that the fiber coiling or bending diameter is highly dependent on the TMI thresholds in multimode fiber amplifiers [35]. Higher TMI threshold can be obtained by further reducing the bend diameter, but too small of a bend diameter will induce a high bend loss of fundamental mode, which will decrease the efficiency and increase the thermal effects. Considering the above factors, the minimum bending diameter for gain fiber is set to 8 cm. Comparing with original coiling shape I of 5 kW NLFA, the shape II or III increases the loss of HOMs by introducing more bending parts. The curvature radius of the adjusted parts ranges from 45 mm to 58 mm.

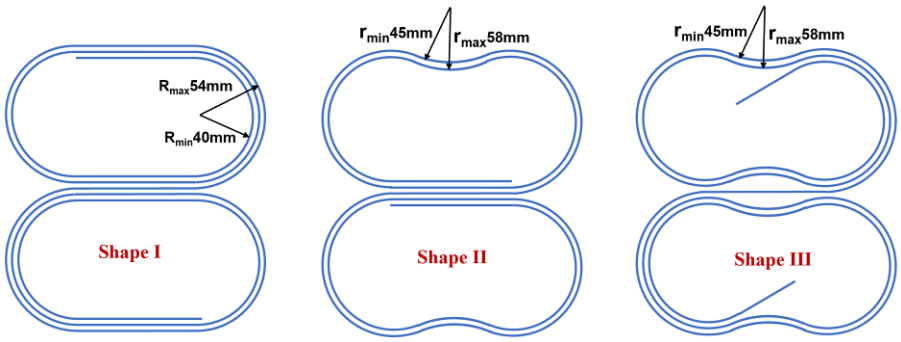

Figure 8. The diagram of coiling shape for gain fiber.

We experimentally investigated the TMI threshold of fiber amplifier with different gain fiber coiling shape. Referring to the pumping ratio of the 5 kW NFLA system, we achieved an output power of 5.5 kW with M^2 factor of 1.35 by employing the coiling shape II for the YDF. The TMI threshold was improved by ~500 W and the optical-optical efficiency did not decrease,

https://doi.org/10.1017/hpl.2024.25 Published online by Cambridge University Press

which demonstrates the coiling method of gain fiber have potential to enhance the output brightness. Furthermore, a final 6040 W NLFA system was obtained by using coiling shape III for the YDF. The total pump power was 7058W with forward and backward pumping ratio of around 1:6.8. Figure 9(a) shows the evolution of output power and optical-to-optical efficiency with the pump power. The conversion efficiency is 85.0% at the maximum power. As shown in Fig. 9 (b), the output spectrum at 6 kW has no sign of FWM and the SNR is 30.25 dB. By integral operation of the spectrum, the Stokes components (1100~1175 nm) take up 1.4% of the total power. The 3 dB and 20 dB linewidth are 0.63 nm and 2.81 nm, respectively. Figure 9 (c) shows the evolution of beam quality with output power. Thanks to the suppression of TMI and SRS effect, the output laser maintained nearly single-mode operation during the power scaling and the beam quality M^2 was ~1.41 at 6 kW. The temporal signal detected by PD and its corresponding FFT spectrum are shown in Fig. 9 (d). The slight frequency fluctuations on FFT spectrum indicates that the NLFA worked around TMI threshold. The maximum backward power monitored from BPFC was about 1.6 W. The laser system withstood 10 minutes of testing and performed stably with the power fluctuation of less than 0.3%.

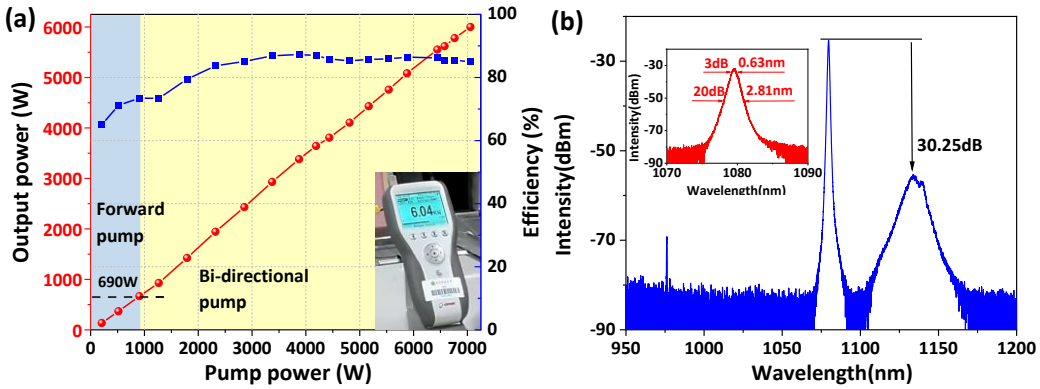

https://doi.org/10.1017/hpl.2024.25 Published online by Cambridge University Press

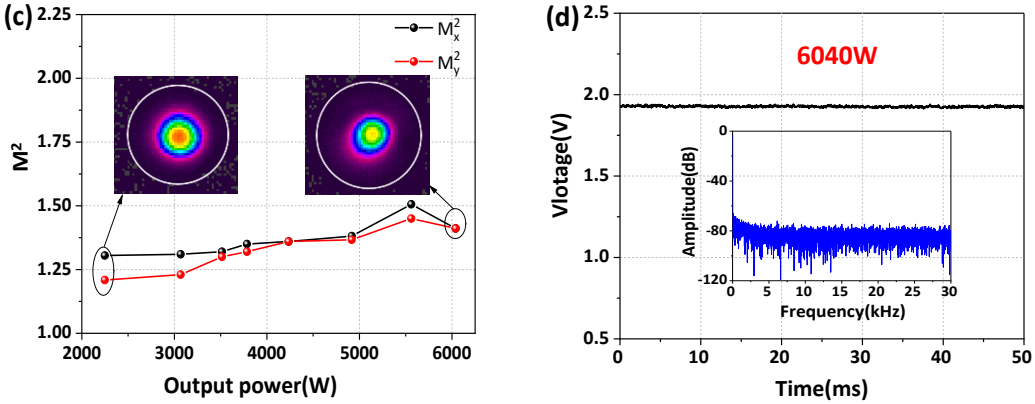

Figure 9. (a) The variation curves of the output laser power and the O-O efficiency with the pump power; (b) The output spectrum at 6 kW; (c) the evolution of beam quality with output power; (d) The signal of the PD at the maximum output power and FFT results.

Figure 10 lists the evolution of laser brightness during the optimization process. By adjusting the bi-directional pumping ratio, various nonlinear effects are mitigated. The laser output power and brightness increase obviously with an enhancement of 90%. With the method of novel coiling for gain fiber, the TMI threshold improves by ~1000 W and laser brightness is further enhanced by a factor of 2.1. Finally, a 6 kW NLFA is achieved with the highest brightness based on the simple MOPA structure.

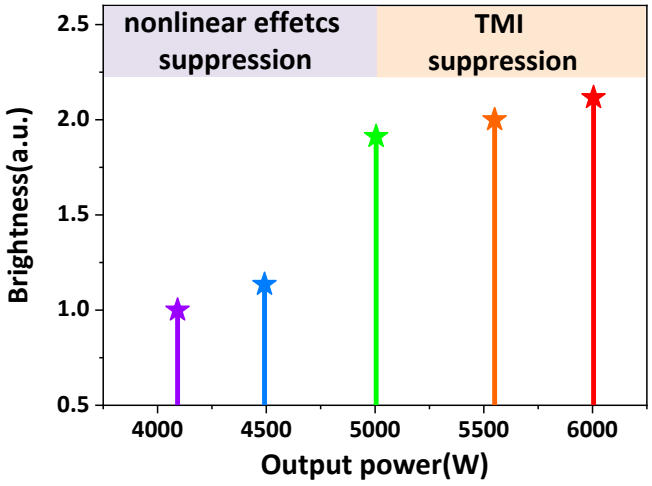

Figure 10. The results of laser brightness enhancement.

https://doi.org/10.1017/hpl.2024.25 Published online by Cambridge University Press

V. CONCLUSION

In conclusion, a near single-mode 6 kW narrow linewidth fiber laser based on simple MOPA structure has been demonstrated for the first time. The methods of optimizing temporal characteristics of FBG-based seed have been adopted by utilizing a novel cavity structure. After decreasing the pumping ratios of amplifier stage, the SRS, FWM, and spectral broadening effects are suppressed simultaneously, so that output power and laser brightness improves together. By adopting a new coiling type for gain fiber of amplifier further, the TMI threshold of system are further improved. The laser brightness is further enhanced by a factor of over 2. Finally, with total pump power of 7058 W (pumping ratio of 1:6.8), a 6-kW fiber laser is achieved with optical-to-optical efficiency of 85.0%. At the maximum output power, the SNR is 30.25 dB and the beam quality M^2 factor is ~1.4. The 3 dB and 20 dB linewidth are 0.63 nm and 2.81 nm, respectively. Overall, this work could provide a good reference for the power scaling of narrow linewidth fiber laser based on the simple MOPA structure. The modified seed structure with optimized temporal characteristics and the novel fiber coiling method are universal for SRS and TMI suppression respectively in traditional fiber amplifier.

Acknowledgement

This work is supported by Science and Technology Innovation Program of Hunan Province (2021RC4027).

References

[1] C. Jauregui, J. Limpert, and A. Tünnermann, “High-power fibre lasers,” Nature Photonics 7, 861 (2013). DOI: https://doi.org/10.1038/nphoton.2013.273.

https://doi.org/10.1017/hpl.2024.25 Published online by Cambridge University Press

[2] D. J. Richardson, J. Nilsson, and W. A. Clarkson, “High power fiber lasers: current status and future perspectives [Invited]”, Journal of the Optical Society of America. B, Optical physics 11, 27 (2010). DOI: https://doi.org/10.1364/JOSAB.27.000B63.

[3] M. N. Zervas, and C. A. Codemard, “High Power Fiber Lasers: A Review”, IEEE J. Sel. Top. Quant. 5, 20 (2014). DOI: https://doi.org/10.1109/JSTQE.2014.2321279.

[4] W. Liu, P. Ma, H. Lv, J. Xu, P. Zhou, and Z. Jiang, “General analysis of SRS-limited high-power fiber lasers and design strategy,” Opt. Express 24(23), 26715–26721 (2016). DOI: https://doi.org/10.1364/OE.24.026715.

[5] J. W. Dawson, M. J. Messerly, R. J. Beach, M. Y. Shverdin, E. A. Stappaerts, A. K. Sridharan, P. H. Pax, J. E. Heebner, C. W. Siders, and C. P. J. Barty, “Analysis of the scalability of diffraction-limited fiber lasers and amplifiers to high average power”, Opt. Express 17, 16 (2008). DOI: https://doi.org/10.1364/OE.16.013240.

[6] T. Eidam, C. Wirth, C. Jauregui, F. Stutzki, F. Jansen, H. J. Otto, O. Schmidt, T. Schreiber, J. Limpert, and A. Tunnermann, “Experimental observations of the threshold-like onset of mode instabilities in high power fiber amplifiers”, Opt. Express 14, 19 (2011). DOI: https://doi.org/10.1364/OE.19.013218.

[7] R. Tao, X. Wang, and P. Zhou, “Comprehensive Theoretical Study of Mode Instability in High-Power Fiber Lasers by Employing a Universal Model and Its Implications," IEEE J. Select. Topics Quantum Electron. 24(3), 1-19 (2018). DOI: https://doi.org/10.1109/JSTQE.2018.2811909.

[8] S. J. McNaught, P. A. Thielen, L. N. Adams, J. G. Ho, A. M. Johnson, J. P. Machan, J. E. Rothenberg, C.-C. Shih, D. M. Shimabukuro, M. P.Wacks, M. E.Weber, and G. D. Goodno, “Scalable Coherent Combining of Kilowatt Fiber Amplifiers Into a 2.4-kW Beam,” IEEE

https://doi.org/10.1017/hpl.2024.25 Published online by Cambridge University Press

Journal of Selected Topics in Quantum Electronics 20(5), 174-181. (2014). DOI: https://doi.org/10.1109/JSTQE.2013.2296771.

[9] Z. Liu, P. Ma, R. Su, R. Tao, Y. Ma, X. Wang, and P. Zhou, "High-power coherent beam polarization combination of fiber lasers: progress and prospect," J. Opt. Soc. Am. B 34, A7-A14 (2017). DOI: https://doi.org/10.1364/JOSAB.34.0000A7.

[10] Y. Zheng, Y. Yang, J. Wang, M. Hu, G. Liu, X. Zhao, X. Chen, K. Liu, C. Zhao, B. He, and J. Zhou, "10.8 kW spectral beam combination of eight all-fiber superfluorescent sources and their dispersion compensation," Opt. Express 24(11), 12063 (2016). DOI: https://doi.org/10.1364/OE.24.012063.

[11] T. Loftus, A. Thomas, P. Hoffman, M. Norsen, R. Royse, A. Liu, and E. Honea, "Spectrally Beam-Combined Fiber Lasers for High-Average-Power Applications," Selected Topics in Quantum Electronics, IEEE Journal of 13, 487–497 (2007). DOI: https://doi.org/10.1109/JSTQE.2007.896568.

[12] A. Flores, C. Robin, A. Lanari, and I. Dajani, "Pseudo-random binary sequence phase modulation for narrow linewidth, kilowatt, monolithic fiber amplifiers," Optics Express 22, (2014). DOI: https://doi.org/10.1364/OE.22.017735.

[13] I. Dajani, A. Flores, R. Holten, B. Anderson, B. Pulford, and T. Ehrenreich, "Multi-kilowatt power scaling and coherent beam combining of narrow-linewidth fiber lasers," Proc of SPIE. 972801 (2016). DOI: https://doi.org/10.1117/12.2218216.

[14] M. Liu, Y. Yang, H. Shen, J. Zhang, X. Zou, H. Wang, L. Yuan, Y. You, G. Bai, B. He, and J. Zhou, "1.27 kW, 2.2 GHz pseudo-random binary sequence phase modulated fiber amplifier with Brillouin gain-spectrum overlap," Sci Rep 10(1), 629 (2020). DOI: https://doi.org/10.1038/s41598-019-57408-5.

[15] C. Yu, O. Shatrovoy, T. Fan, and T. Taunay, “Diode-pumped narrow linewidth multi-kilowatt metalized Yb fiber amplifier,” Opt. Lett. 41(22), 5202–5205 (2016). DOI: https://doi.org/10.1364/ol.41.005202.

[16] A. Harish and J. Nilsson, “Optimization of phase modulation with arbitrary waveform generators for optical spectral control and suppression of stimulated Brillouin scattering,” Opt. Exp. 23(6), 6988–6999 (2015). DOI: https://doi.org/10.1364/OE.23.006988.

[17] Z. Huang, Q. Shu, R. Tao, Q. Chu, Y. Luo, D. Yan, X. Feng, Y. Liu, W. Wu, H. Zhang, H. Lin, J. Wang, and F. Jing, “>5kW Record High Power Narrow Linewidth Laser from Traditional Step-Index Monolithic Fiber amplifier,” Photonics Technology Letters, 33(21), 1181-1184 (2021). DOI: https://doi.org/10.1109/LPT.2021.3112270.

[18] G. Wang, J. Song, Y. Chen, S. Ren, P. Ma, W. Liu, T. Yao, and P. Zhou, “Six kilowatt record all-fiberized and narrow-linewidth fiber amplifier with near-diffraction-limited beam quality,” High Pow Laser Sci Eng 10, e22 (2022). DOI: https://doi.org/10.1017/hpl.2022.12.

[19] P. Ma, T. Yao, Y. Chen, G. Wang, S. Ren, W. Li, W. Liu, Z. Pan, L. Huang, Z. Chen, P. Zhou, J. Chen, “New progress of high-power narrow-linewidth fiber lasers,” Proceedings of SPIE 12310, Advanced Lasers, High-Power Lasers, and Applications XIII. 2022: 123100E (2022). DOI: https://doi.org/10.1117/12.2643929.

[20] Y. Huang, Q. Xiao, D. Li, J. Xin, Z. Wang, J. Tian, Y. Wu, M. Gong, L. Zhu, and P. Yan, “3 kW narrow linewidth high spectral density continuous wave fiber laser based on fiber Bragg grating,” Optics & Laser Technology 133, 106538 (2021). DOI: https://doi.org/10.1016/j.optlastec.2020.106538.

[21] S. Du, G. Fu, T. Qi, C. Li, Z. Huang, D. Li, P. Yan, M. Gong, and Q. Xiao, "3.3 kW narrow linewidth FBG-based MOPA configuration fiber laser with near-diffraction-limited beam

https://doi.org/10.1017/hpl.2024.25 Published online by Cambridge University Press

quality," Optical Fiber Technology 73, 103011 (2022). DOI: https://doi.org/10.1016/j.yofte.2022.103011.

[22] X. Tian, B. Rao, X. Xi, M. Wang, C. Wang, and Z. Wang, "Selection principle of seed power in high-power narrow linewidth fiber amplifier seeded by a FBGs-based fiber oscillator," Opt. Express 31(8), 12016 (2023). DOI: https://doi.org/10.1364/OE.479144.

[23] S. Liao, T. Luo, R. Xiao, C. Shu, J. Cheng, Z. Zhang, Y. Xing, H. Li, N. Dai, and J. Li, "4.6 kW linearly polarized and narrow-linewidth monolithic fiber amplifier based on a fiber oscillator laser seed," Opt. Lett. 48(24), 6533 (2023). DOI: https://doi.org/10.1364/OL.507009.

[24] A. E. Bednyakova, O. A. Gorbunov, M. O. Politko, S. I. Kablukov, S. V. Smirnov, D. V. Churkin, M. P. Fedoruk, and S. A. Babin, "Generation dynamics of the narrowband Yb-doped fiber laser," Opt. Express 21(7), 8177-8182 (2013). DOI: https://doi.org/10.1364/OE.21.008177.

[25] W. Liu, P. Ma, H. Lv, J. Xu, P. Zhou, and Z. Jiang, "General analysis of SRS-limited high-power fiber lasers and design strategy," Opt. Express 24(23), 26715 (2016). DOI: https://doi.org/10.1364/OE.24.026715.

[26] W. Liu, P. Ma, H. Lv, J. Xu, P. Zhou, and Z. Jiang, "Investigation of stimulated Raman scattering effect in high-power fiber amplifiers seeded by narrow-band filtered superfluorescent source," Opt. Express 24(8), 8708 (2016). DOI: https://doi.org/10.1364/OE.24.008708.

[27] S. Zhang, W. Zhang, M. Jiang, W. Liu, P. Ma, C. Li, R. Su, P. Zhou, and Z. Jiang, "Suppressing stimulated Raman scattering by adopting a composite cavity in a narrow

https://doi.org/10.1017/hpl.2024.25 Published online by Cambridge University Press

linewidth fiber oscillator," Appl. Opt. 60(20), 5984 (2021). DOI: https://doi.org/10.1364/AO.430054.

[28] W. Liu, P. Ma, and P. Zhou, "Unified model for spectral and temporal properties of quasi-CW fiber lasers," J. Opt. Soc. Am. B 38(12), 3663 (2021). DOI: https://doi.org/10.1364/JOSAB.439829.

[29] T. Li, W. Ke, Y. Ma, Y. Sun, and Q. Gao, "Suppression of stimulated Raman scattering in a high-power fiber amplifier by inserting long transmission fibers in a seed laser," Journal of the Optical Society of America B 36(6), 1457 (2019). DOI: https://doi.org/10.1364/JOSAB.36.001457.

[30] X. Tian, B. Rao, M. Wang, X. Xi, C. Wang, W. Liu, P. Ma, Z. Chen, H. Xiao, H. Fang, and Z. Wang, "A Novel Structure for Raman Suppression in Narrow Linewidth Fiber Amplifier," IEEE Photon. Technol. Lett. 35(21), 1175–1178 (2023). DOI: https://doi.org/10.1109/LPT.2023.3307657.

[31] V. Bock, A. Liem, T. Schreiber, R. Eberhardt, A. Tünnermann, "Explanation of stimulated Raman scattering in high power fiber systems", in: A.L. Carter, I. Hartl (Eds.), Fiber Lasers XV: Technology and Systems, SPIE, San Francisco, United States, 2018: p. 50. DOI: https://doi.org/10.1117/12.2287770.

[32] H. Xu, M. Jiang, P. Zhou, G. Zhao, and X. Gu, "Elimination of self-mode-locking pulses in high-power continuous-wave Yb-doped fiber lasers with external feedback," Appl. Opt. 56(32), 9079 (2017). DOI: https://doi.org/10.1364/AO.56.009079.

[33] C. Zhang, R. Tao, M. Li, X. Feng, R. Liao, Q. Chu, L. Xie, H. Li, B. Shen, L. Xu, and J. Wang, "Theoretical Analysis of the Mode Distortion Induced by Stimulated Raman

https://doi.org/10.1017/hpl.2024.25 Published online by Cambridge University Press

Scattering Effect in Large-Mode Area Passive Fibers," J. Lightwave Technol. 41(2), 671–677 (2023). DOI: https://doi.org/10.1109/JLT.2022.3215659.

[34] C. Zhang, L. Xie, H. Li, B. Shen, X. Feng, M. Li, R. Tao, and J. Wang, "SRS-Induced Spatial-Spectral Distortion and Its Mitigation Strategy in High-Power Fiber Amplifiers," IEEE Photonics J. 14(2), 1–5 (2022). DOI: https://doi.org/10.1109/JPHOT.2022.3149348.

[35] F. Zhang, H. Xu, Y. Xing, S. Hou, Y. Chen, J. Li, N. Dai, H. Li, Y. Wang, and L. Liao, "Bending diameter dependence of mode instabilities in multimode fiber amplifier," Laser Physics Letters 16, 035104 (2019). DOI: https://doi.org/10.1088/1612-202X/aaff4b.

https://doi.org/10.1017/hpl.2024.25 Published online by Cambridge University Press